Failure Surfaces for the Design of Ceramic-Lined Gun Tubes

Robert Carter
U.S. Army Research Laboratory
Aberdeen Proving Ground, MD 21005

ABSTRACT

It is desired to incorporate advanced materials in gun barrels to increase service life, enable advanced propellants to provide for increased kinetic energy, and decrease system weight. Ceramic materials possess superior erosion resistance, high temperature performance, and lower density than steel making them attractive candidates as gun tube liners. A new design approach is necessary to address the large variability in strength, one that is probabilistic instead of deterministic in nature. Models derived to incorporate this new approach have been developed and are being used to provide an understanding of the optimal geometry, sheathing material requirements, and pre-stress levels for system success.

BACKGROUND and MODEL DEVELOPMENT

Ceramic materials are being investigated as bore materials for high performance gun barrels. Their superior high temperature behavior and hardness result in reduced erosion rates, when compared to gun steels, and make them strong candidates for application in the harsh environment produced during a ballistic event. Previous ceramic gun barrel attempts have met with limited success, at best, but advances in ceramic material processing, probabilistic design, and sheathing technologies have prompted the U. S. Army Research Laboratory to investigate ceramic materials anew[1,2,3,4,5,6,7]. The primary limiting factors in the past have been the inability to design around the inherent low tensile strength, large variability in the observed strength, and brittle failure.

Statistical methods are necessary to design around the variability in observed strength of ceramic components. The most recognized approach is the assumption that a Weibull distribution of strength-limiting flaws exists in the material. The original Weibull equation calculates a probability of failure (P_f) for a brittle material subjected to a uniform and uniaxial stress distribution and may be expressed as:

$$P_f = 1 - e^{-\int \left(\frac{\sigma}{\sigma_o}\right)^m dV} \quad (1)$$

with σ being the stress, σ_o the Weibull strength or scale parameter, and m being the Weibull modulus. This expression only considers one type of flaw population located in the volume of the ceramic body subjected to a uniform stress[8]. For a pressurized tube, additional conditions need to be evaluated, namely the probability for a nonuniform stress state and multiple flaw populations[9]. The nonuniform stress changes Equation 1 into:

$$P_{fV} = 1 - e^{-k_V V \left(\frac{\sigma_{\max}}{\sigma_{oV}}\right)^{m_V}} \quad (2)$$

where

$$k_V V = \int \left(\frac{\sigma(r)}{\sigma_{\max}}\right)^{m_V} dV \quad (3)$$

P_{fV} is the probability of failure due to a volumetric flaw, $k_V V$ is the effective volume, $\sigma(r)$ is the stress distribution function, σ_{max} is the maximum stress in the volume, and σ_{oV} and m_V are the Weibull strength and scale parameters for the volumetric flaw. Similar expressions for surface flaws have been derived in the literature[9]. In order to address multiple flaw populations of volume, surface, and the possibility of multiples of each, the new total probability of failure becomes:

$$P_f = 1 - \prod_{i=1}^{N} \left(1 - P_{fi}\right) \quad (4)$$

Where P_f is the combined or total probability of failure, and P_{fi} is the probability of failure due to the i^{th} (out of N) flaw type.

Currently, the strength of structural ceramics is not sufficient to support the ballistic pressure load generated during firing. In order to increase the rupture pressure, the ceramic must be compressively pre-stressed. To model the multi-

Report Documentation Page

Form Approved
OMB No. 0704-0188

1. REPORT DATE	2. REPORT TYPE	3. DATES COVERED
00 DEC 2004	**N/A**	**-**

4. TITLE AND SUBTITLE	5a. CONTRACT NUMBER
Failure Surfaces for the Design of Ceramic-Lined Gun Tubes	5b. GRANT NUMBER
	5c. PROGRAM ELEMENT NUMBER
6. AUTHOR(S)	5d. PROJECT NUMBER
	5e. TASK NUMBER
	5f. WORK UNIT NUMBER
7. PERFORMING ORGANIZATION NAME(S) AND ADDRESS(ES) **U.S. Army Research Laboratory Aberdeen Proving Ground, MD 21005**	8. PERFORMING ORGANIZATION REPORT NUMBER
9. SPONSORING/MONITORING AGENCY NAME(S) AND ADDRESS(ES)	10. SPONSOR/MONITOR'S ACRONYM(S)
	11. SPONSOR/MONITOR'S REPORT NUMBER(S)

12. DISTRIBUTION/AVAILABILITY STATEMENT
Approved for public release, distribution unlimited

13. SUPPLEMENTARY NOTES
See also ADM001736, Proceedings for the Army Science Conference (24th) Held on 29 November - 2 December 2005 in Orlando, Florida. , The original document contains color images.

14. ABSTRACT

15. SUBJECT TERMS

16. SECURITY CLASSIFICATION OF:			17. LIMITATION OF ABSTRACT	18. NUMBER OF PAGES	19a. NAME OF RESPONSIBLE PERSON
a. REPORT	b. ABSTRACT	c. THIS PAGE			
unclassified	**unclassified**	**unclassified**	**UU**	**6**	

Standard Form 298 (Rev. 8-98)
Prescribed by ANSI Std Z39-18

layered design of the ceramic and sheathing material and to calculate the stress distributions, the probability of failure equations need to be coupled with a model capable of describing the response of the structure. This work utilized the model developed by Rousseau, *et al.*, 1987; for calculating the stress, strain, and displacement of an N-ply anisotropic laminated tube[10,11]. The model can be used to determine the stress levels generated by different pre-stress methods, such as, shrink-fit, press-fit, and high-tension filament winding. Modifications to the strain term in the constitutive equations are necessary to represent the different pre-stress conditions. The strain expression becomes:

$$\varepsilon = \varepsilon^{E} - \varepsilon^{Th} + \varepsilon^{w} + \varepsilon^{INT} \qquad \textbf{(5)}$$

where ε is the total strain, ε^{E} is the elastic strain, and ε^{Th} is the thermal strain ($\alpha\Delta T$). The ε^{W} term is the elastic strain stored due to the tensile load applied to the fibers during filament winding[12]. The ε^{INT} term is the strain due to the amount of interference imparted by a press-fit operation.

MODEL VERIFICATION

The model development has coincided with experimental testing to provide a means for verification. Initial tests were of unsheathed or blank ceramic tubes. Due to the variable nature of the strength values the predictions provide ranges where there is a high probability of failure, as opposed to a specific value. Numerous tests have been conducted in order to determine the Weibull properties of several candidate ceramic materials[13]. Material properties for two of the silicon nitride materials used for experimental testing are listed in Table 1.

Table 1 - Material properties for two silicon nitride compositions

Property	SN47	SN5P
Modulus (GPa)	326	313
Poisson's Ratio	0.26	0.25
CTE (ppm/°C)	3.18	3.19
σ_{oV} (MPa*mm$^{3/m}$)	1653	887
m_v	9.4	16.9
σ_{oA} (MPa*mm$^{2/m}$)	1047	949
m_A	13.7	12.3

The tests have characterized volumetric flaws and two types of surface flaws on the outer surface, but none have been conducted on the inner surface. In order to get around this lack of information, the inner surface will be treated as if it contains identical flaw populations as the outer surface. This assumption is not ideal, but allows for high and low estimates of the probability of failure for a given sample. In Figure 1 there are two curves showing the probability of failure for the SN47 silicon nitride tube (24 ID x 33mm OD x 50mm long). The lower estimate is for the combined probability of failure for surface and volumetric flaws. The higher estimate was calculated using a probability of failure due to volumetric flaws only. In between these two curves are the experimental data for burst pressure for different silicon nitride tubes. At the time of this publication there have been eight tests of the unsheathed tubes. The results have been ranked as described in the ASTM standard for determining the Weibull characteristics[14]. Even though there are a small number of data points, the data appears to be well bracketed by the different predictions curves.

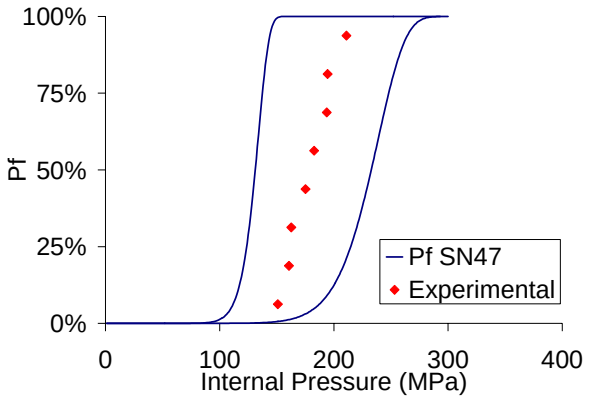

Figure 1 - High and low predictions for the burst pressure for unsheathed SN47 silicon nitride tube.

The next application was using the model to predict the burst pressure for a sheathed ceramic tube. Several tubes have been fabricated using high tension filament wrapping to create a composite sheath onto the ceramic tubes. A plot of the result of one of the silicon nitride tubes is in Figure 2. Again, the two different prediction curves for the different assumptions are shown as smooth curves, while the burst pressure is highlighted using a vertical dashed line. Since there is only one data point it is impossible to rank the value and give it a single probability of failure value. Again the data appears to be well predicted by the model results.

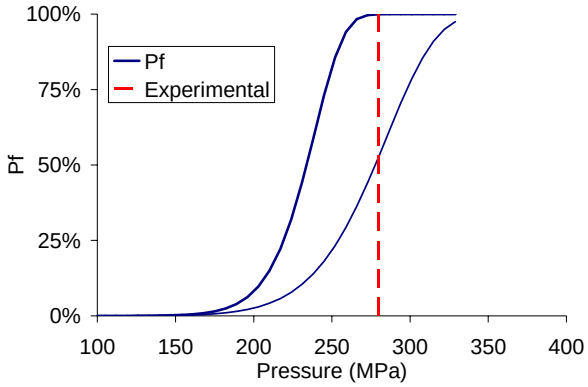

Figure 2 - High and low predictions for the burst pressure for a filament wound composite sheathed silicon nitride tube (SN47).

Further development of the experimental tests has progressed to ballistic simulation via live firing through the tube, as seen in Figure 3. A ballistic fixture was used to mate the composite wrapped ceramic tube to a gun chamber. Special projectiles were developed to fit within the 24mm ID, and varying propellant changes were used to incrementally subject the barrel to higher pressure loadings. In Figure 4, the model predictions for the probability of failure are plotted against the pressure produced in the ballistic test fixture. It should be noted that the sample was removed after the last shot at 262 MPa when it appeared to have a crack. Upon further inspection, the sample was still intact and had not failed.

Figure 3 – Overwrapped ceramic tube for ballistic testing.

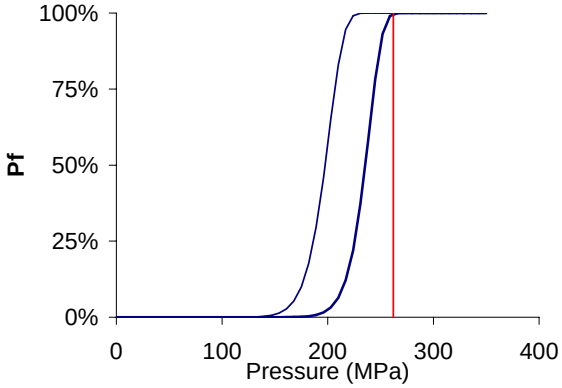

Figure 4 - High and low predictions for a composite/silicon nitride tube (SN5P) in a ballistic test fixture.

FAILURE SURFACES

With the successes of the predictions for the failure pressure ranges for both unsheathed and sheathed tubes, it is reasonable to use the model to investigate barrel designs for actual gun systems. Having established the failure criterion for the ceramic liner as the Weibull probability of failure, the need for a suitable failure criterion for the sheathing materials remains. The criterion has to be tailored to the sheathing material, in that, composite materials use different criterion than metals. For this study the metal jackets will be represented using a von Mises yielding criterion. While this does not represent the ultimate strength of the material, it does represent an end to where this model can accurately represent the material response. Once a metal jacket yields due to a pressure load, the pre-stress will redistribute and change the load on the ceramic. Due to this, the model will be limited to just the elastic response of the system and not beyond the yield points of the sheath. For composite sheathes, a different criterion will be employed. Since most of the sheathes are hoop wound, or employ an angle very close to an all-hoop winding, the primary stress will be in the fiber direction. For this situation a maximum tensile stress criterion will be employed. For the remaining calculations and plots, the sheath materials will be steel and a carbon fiber composite. The mechanical properties for the materials are listed in Table 2.

Table 2 - Typical sheath material properties[15]

Property	Steel	Composite
E_{11} (GPa)	200	148
$E_{22}=E_{33}$ (GPa)	200	10.5
G_{12} (GPa)	76	5.61
$\nu_{12} = \nu_{13}$	0.32	0.3
ν_{23}	0.32	0.59
α_{11} (ppm/°C)	12.8	-0.8
$\alpha_{22}= \alpha_{33}$ (ppm/°C)	12.8	29
Strength value (MPa)	1103	2137

It becomes very attractive to investigate optimal design spaces by parametric studies on tube geometry, pre-stress levels, and sheathing. By selecting a fixed wall thickness and varying the ceramic and sheathing wall thickness ratio and pre-stress level, optimal design spaces are illustrated by the lowest probability of failure in the ceramic without failing the sheath. Pre-stress can be varied by changing the temperature for shrink-fit applications, wind tension for over-wrapped composite designs, or interference mismatch for press-fit operations.

The plots are formed from the competing failure criteria for a pressurized tube. The probability of failure calculations range from 1 to zero, so it is more useful to present them on a logarithmic scale plot. In order to differentiate between the different criteria, the failure value is artificially inflated when the stress in the sheath exceeds the peak stress or Von Mises value. The plot in Figure 5 is a cross section of a failure surface. The x-axis is the interference mismatch between the ceramic and the sheath. The y-axis is the log of the probability of failure. The two curves are for different ratios of ceramic thickness to total wall thickness. The curves on the right half of the plot (interference strain between 0 and -0.004) have values less than zero indicating the sheath is intact and the survival is governed by the ceramic. When the interference is increased (the left half of the plot) the stress levels in the sheath increase and the sheath begins failing, as seen by the jump to values greater than zero. For this example, the design with the ceramic ratio of 25% is the better design. The design exhibits a lower probability of failure over a larger range of interference.

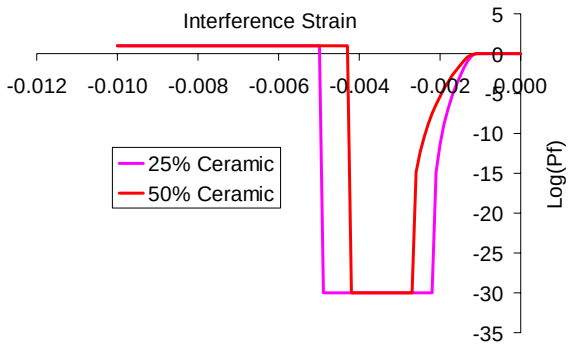

Figure 5 – Probability of failure curves for a sheathed tube

A parametric surface where both the pre-stress level and wall thickness ratio are varied will illustrate the optimal design geometry and pre-stress level. An example of this is in Figure 6. It is the equivalent of looking down on the plot in Figure 5. Instead of showing the depth of the plot it has been color coded to identify the different regions of the plot. The yellow region is the area where the ceramic would probably fail (Pf is between 1 and 1 in 1 million). The green area is where the sheath is over-stressed and fails. The maroon and blue regions are areas of probable success (Pf less than 1 in 1 million). As can be seen in Figure 6 and Figure 7 both sheathing approaches generate a region of probable success for a range of thickness ratios and pre-stress levels for a 5.56mm barrel.

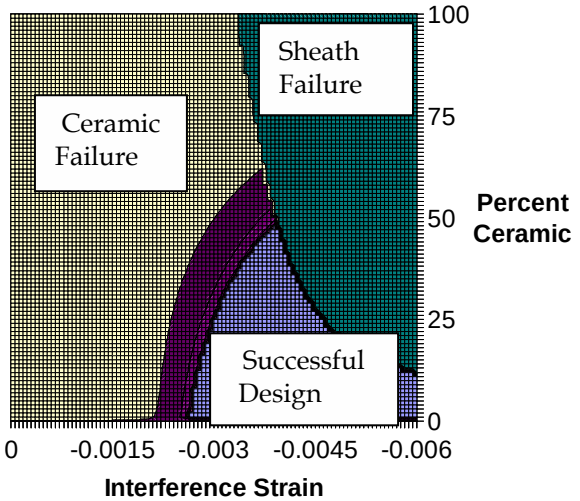

Figure 6 - Failure surface for an interference fit for a steel sheathed, silicon nitride 5.56mm barrel.

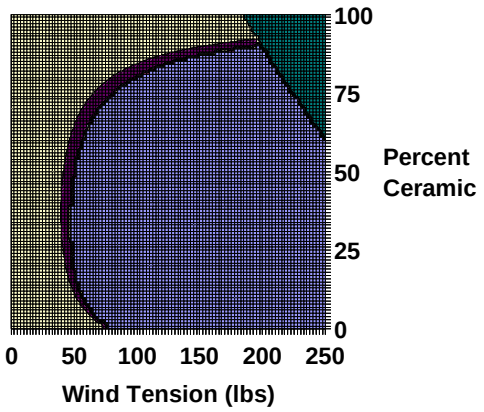

Figure 7 – Failure surface for a high tension filament wound composite and silicon nitride 5.56mm barrel.

These model predictions have been applied to a range of calibers. The most demanding of the large caliber systems is the 120mm tank cannon, due to the larger size and high ballistic pressures. The surface plotted in Figure 8 is of a steel jacketed ceramic tube for use in the 120mm system. There is not a combination of pre-stress level and wall thickness ratio that has a significant probability of success. For the high tension filament wound composite system, as seen in Figure 9, there is still a successful region.

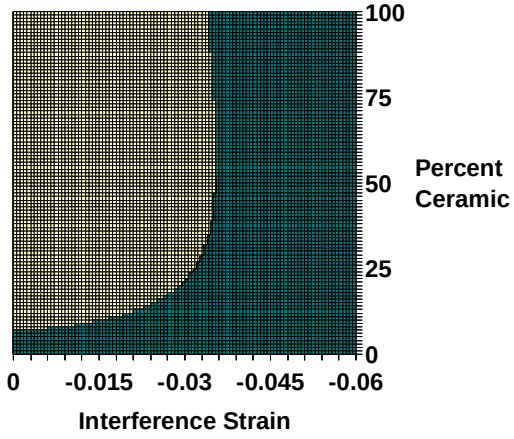

Figure 8 – Failure Surface for an interference-fit steel sheath on a silicon nitride gun tube for a 120mm cannon.

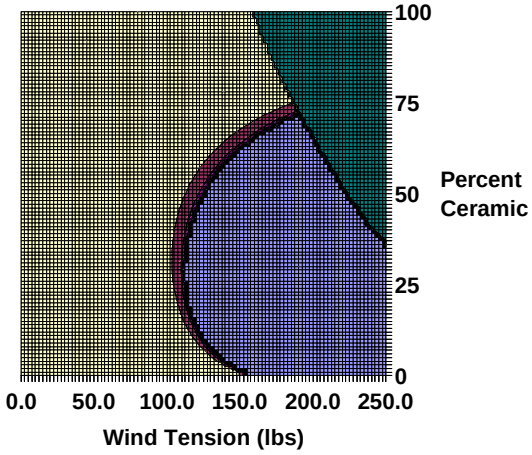

Figure 9 – Failure surface for filament wound composite sheathed silicon nitride tube for a 120mm cannon.

It should be noted that the interference models used in this paper are for a single layer design. By increasing the number of layers where each layer has its own interference-fit with the other layers, a design space arises for a 120mm steel/silicon nitride system, as can be seen in Figure 10. The total thickness is the same for this model as in Figure 8, but it includes four different steel layers that are interference-fit with each preceding layer. The difference in the x-axis is that with the different layers it is necessary to control the layer stress levels rather than the interference amount. The sheath failure region is now a vertical line since the x-axis is the Von Mises stress at each layer, so all the layers fail when the layers reach the failure criterion.

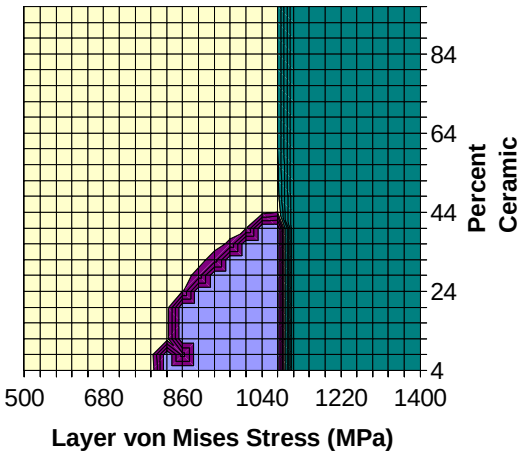

Figure 10 – Failure surface for a multi-layered interference fit steel sheath on a silicon nitride gun tube for a 120mm cannon.

DISCUSSION AND CONCLUSIONS

This model illustrates that with the optimal design conditions a ceramic lined gun can successfully function. Investigations into different sheathing materials, geometries, operating conditions, fabrication methods, and material properties are all possible, and have been performed for various caliber gun systems and candidate material systems. While this approach generates plots for the static case at one point along a barrel's length, it does not consider dynamic effects or thermal gradients that are present in gun systems. Because of this, the model is being used as a screening tool, since it is successful at determining what starting design parameters should be pursued with finite element and other engineering design software capable of capturing the dynamic thermo-mechanical stresses. Once more accurate models have been created, software, such as NASA's CARES code, can perform the probabilistic analysis of the stress states from the finite element analysis.

The model results and experimental verification provide strong support for developing and designing ceramic lined gun barrels. Further investigations into erosion rates, thermal shock resistance, sheathing technology, and fabrication issues are being pursued in order to develop a system capable of increased service life, increased kinetic energy, and decreased weight for the warfighter.

REFERENCES

[1] R. Harlow and R. Kimball, *Composite Barrel Materials Research and Development*, Air Force Armament Laboratory Technical Report AFATL-TR-72-3, Eglin Air Force Base, Florida, January 1972.

[2] R. Harlow, W. Briggs, and R. Kimball, *Development of Full Length, Insulated Composite Barrels for Aircraft Machine Guns*, Air Force Armament Laboratory Technical Report AFATL-TR-73-10, Eglin Air Force Base, Florida, January 1973.

[3] S. Fischman and C. Palmer, *The Design and Fabrication of a Ceramic-Lined Gun Barrel Insert*, Naval Surface Weapons Center/Dahlgren Laboratory Technical Report TR-3342, Dahlgren, Virginia, July 1975.

[4] G. D'Andrea, R. Cullinan, and P. Croteau, *Refractory Lined Composite Pressure Vessels*, Technical Report ARLCB-TR-78023, U. S. Army Armament Research and Development Command, Benet Weapons Laboratory, Watervliet, New York, December 1978.

[5] R. Giles, E. Bunning, and D. Claxton, *Feasibility of Ceramic Lined Gun Tube*, U. S. Army Armament Research and Development Command Report ARLCD-CR-80058, prepared by Maremont Corporation, Saco, Maine, February 1981.

[6] P. Stephan and A. Rosenfield, *Survey of Ceramics in Gun Barrels*, Report AMMRC SP-82-1, Materials Technology Laboratory, Watertown, Massachusetts, 1982.

[7] R. Katz, *Ceramic Gun Barrel Liners: Retrospect and Prospect*, Proceedings of the Sagamore Workshop on Gun Barrel Wear and Erosion sponsored by the Army Research Laboratory, Wilmington, DE, July 1996.

[8] W. Weibull, "A Statistical Theory of the Strength of Materials," *Proceedings of the Royal Swedish Institute of Engineering Research*, No. 151, 1-45, 1939.

[9] R. Carter, "Model Development for Parametric Design of Pressurized Ceramic Tubing" *Ceramic Engineering and Science Proceedings*, Vol. 24, Issue 4, pp 477-482, 2003.

[10] C. Rousseau, Master's Thesis: "Stresses and Deformations in Angle-Ply Composite Tubes," Virginia Tech, Blacksburg, VA, 1987.

[11] C. Rousseau, M. Hyer, and S. Tompkins, "Stresses and Deformations in Angle-Ply Composite Tubes," CCMS-87-04, Virginia Tech, Blacksburg, VA, 1987.

[12] R.F. Eduljee and J. W. Gillespie, "Elastic Response of Post- and In Situ Consolidated Laminated Cylinders"; *Composites: Part A*, **27**A, 437-446, 1996.

[13] J. J. Swab, A. Wereszczak, J. Tice, R. Caspe, R. Kraft, and J. Adams, "Mechanical and Thermal Properties of Advanced Ceramics for Gun Barrel Applications", Army Research Laboratory Technical Report, *In Press*.

[14] ASTM C1239-00, "Standard Practice for Reporting Uniaxial Strength Data and Estimating Weibull Distribution Parameters for Advanced Ceramics", 2004 Annual Book of ASTM Standards, Vol. 15.01.

[15] C. T. Herakovich, *Mechanics of Fibrous Composites*, John Wiley & Sons, New York, 1998, p. 14.